

Path-integral approach to Debye–Waller factors in EXAFS, EELS and XPD for cubic and quartic anharmonic potentials

Takafumi Miyanaga,^{a*} Toshiyuki Suzuki^b and Takashi Fujikawa^b

^a*Faculty of Science and Technology, Hirosaki University, Bunkyo-cho 3, Hirosaki, Aomori 036-8561, Japan, and* ^b*Graduate School for Science, Chiba University, Yayoi-cho 1-33, Inage-ku, Chiba 263-8522, Japan. E-mail: takaf@cc.hirosaki-u.ac.jp*

(Received 13 April 1999; accepted 15 November 1999)

In this paper thermal effects in extended X-ray absorption fine structure (EXAFS) and X-ray photoelectron diffraction (XPD) due to atomic vibration in cubic and quartic potentials are studied by use of Feynman's path-integral approach. This approach can be applied to strongly anharmonic systems where the cumulant analyses break down. It is closely related to the well known classical approach which is only valid at high temperature. The phase of the thermal factor plays an important role both in EXAFS and XPD analyses for the asymmetric potential with strong anharmonicity. At low temperature the cumulant expansion up to the second order for the thermal damping function agrees well with the self-consistent result, but up to higher orders should be taken into account for the phase function. At high temperature the result from self-consistent calculations shows the characteristic behaviour: the thermal damping function is negative in the high- k region for both strongly and weakly anharmonic systems. The cumulant approximation cannot reproduce this behaviour. For the strongly anharmonic systems the quantum result shows qualitatively different behaviour from the classical approximation at low temperature: the former does not show the negative values even in the high- k region, while the latter shows the phase inversion in the amplitude.

Keywords: EXAFS; X-ray photoelectron diffraction; Debye–Waller factors; path integrals; cumulant expansion; anharmonic vibration.

1. Introduction

Theoretical aspects of temperature dependence in extended X-ray absorption fine structure (EXAFS) were first studied by Beni & Platzman (1976) within the framework of harmonic vibration for nuclear motion and plane-wave approximation for photoelectron waves. Since that time some improvements have been found beyond the harmonic approximation (Tranquada & Ingalls, 1983; Fujikawa & Miyanaga, 1993; Miyanaga & Fujikawa, 1994*a,b*; Yokoyama *et al.*, 1996*a,b*; Ishii, 1992) and the plane-wave approximation (Brouder, 1988; Brouder & Goulon, 1989; Rennert, 1992, 1993; Fujikawa *et al.*, 1995, 1998; Yanagawa & Fujikawa, 1996*a*; Yimagawa & Fujikawa, 1996). In order to include the anharmonic effects in the EXAFS analyses, perturbation theory has been applied by use of temperature Green's function or thermal perturbation theory. The former approach has been applied to infinite crystals and the latter to finite clusters in solids. These perturbation approaches are useful for describing weak anharmonicity in the analyses of temperature effects in EXAFS, electron energy-loss spectroscopy (EELS) and X-ray photoelectron diffraction (XPD) spectra, and they have provided interesting information based on cumulant expansion.

On the other hand, the real-space classical approach proposed by Yokoyama *et al.* (1989) has been widely used to relate the EXAFS Debye–Waller factors to interatomic potential. Dalba *et al.* have extensively applied the real-space classical approach to the thermal factor in EXAFS for AgI (Dalba *et al.*, 1995), and to other systems (Dalba *et al.*, 1998). Stern *et al.* (1991) performed the anharmonic analysis of the EXAFS for liquid Pb, and Baberschke and co-workers studied the anharmonicity on the surface by EXAFS (Arvanitis *et al.*, 1993; Rabus *et al.*, 1991). The classical approximation can be safely used in the high-temperature region even though the anharmonicity is strong (Fujikawa & Miyanaga, 1993). Frenkel & Rehr (1993) related XAFS cumulants with the thermal expansion quantum mechanically.

Recently, we have derived general expressions for the Debye–Waller factors in EXAFS, EELS and XPD based on the perturbation theory by use of temperature Green's function, and have applied these to one-dimensional crystals (Fujikawa & Miyanaga, 1993; Miyanaga & Fujikawa, 1994*a,b*). Basically they are based on perturbation theory, and their applicability is restricted to weakly anharmonic systems.

The previous paper (Fujikawa *et al.*, 1997) describes a real-space approach to the EXAFS thermal factor analyses

based on the finite-temperature path-integral method originally developed by Feynman (1972) and improved by Cuccoli *et al.* (1995) and Feynman & Kleinert (1986). This approach without use of the perturbation theory can be applied to strongly anharmonic systems and can be closely related to the classical formulae, so we can study the range of the applicability of the widely used cumulant analyses and of the classical approximation for the study of EXAFS thermal factors. This kind of study is important and basic for the EXAFS, EELS and XPD analyses. In the previous paper (Fujikawa *et al.*, 1997) we pointed out the breakdown of the cumulant expansion for a double-well potential, which can be observed as an unexpected phase inversion of the EXAFS oscillation (Mustre de Leon *et al.*, 1992). More recently we applied the path-integral approach to the analyses of XPD and EXAFS thermal factors of diatomic systems vibrating in the Morse potential in thermal equilibrium at temperature T (Miyana & Fujikawa, 1998). The Morse potential can describe dissociation processes because of asymmetry, so that it is important to study the EXAFS thermal factors for this anharmonic dissociative potential both from chemical and physical interests. The Morse potential is asymmetric and the phase factors should also be influenced by the thermal vibration; therefore it is interesting to study the strongly anharmonic effects on the EXAFS and XPD phase factors. Yokoyama (1998) applied the path-integral method to EXAFS analyses for the Br_2 diatomic molecule which can be considered as a model with cubic and quartic anharmonic potential. He showed that the effective potential method based on the path-integral technique reproduces well the experimental second, third and fourth cumulants.

In this paper we apply the path-integral approach to the EXAFS and the XPD thermal factors of diatomic systems vibrating with additional cubic and quartic anharmonic potential which are in thermal equilibrium at temperature T . This potential is asymmetric and the result can be compared with the previous result for the Morse potential.

2. Basic theory

Let us consider diatomic systems in a reservoir at temperature T whose relative vibrational motion is described by the Hamiltonian

$$H = (p^2/2\mu) + V(q), \quad (1)$$

where μ is the reduced mass and q is the instantaneous interatomic distance. When we deal with the statistical average of an operator A , we should calculate the trace,

$$\langle A \rangle = \text{Tr}(A\rho)/Z, \quad (2)$$

where ρ is the density operator defined by

$$\rho = \exp(-\beta H), \quad (3)$$

where $\beta = 1/k_B T$ and

$$Z = \exp(-\beta F) = \text{Tr}(\rho) \quad (4)$$

is the partition function for the system. The trace can be calculated by applying Feynman's path-integral techniques. However, instead of summing over all paths in just one step, one can classify the paths into two groups as proposed by Feynman (1972). One group consists of an average (quasi classical) path given by

$$\bar{q} = \int_0^\beta du q(u)/\beta, \quad (5)$$

and the other group consists of quantum fluctuation around \bar{q} . The average path is the same as the classical path in the high-temperature limit ($\beta \rightarrow 0$). To use the non-perturbation method based on the path-integral technique we approximate the instantaneous potential $V[q(u)]$ by a trial potential quadratic in the fluctuation path (Cuccoli *et al.*, 1995; Feynman & Kleinert, 1986),

$$V \simeq V_0(q, \bar{q}) = w(\bar{q}) + \mu\omega(\bar{q})^2(q - \bar{q})^2/2. \quad (6)$$

Now the parameters $w(\bar{q})$ and $\omega(\bar{q})$ are to be optimized so that the trial reduced density well approximates the true reduced density. A variational approach which gives the same result as the self-consistent approximation is also possible. The final expression for the average of a local operator A can be represented in terms of the probability density just like classical statistical mechanics (from now on q is used instead of \bar{q} for brevity),

$$\langle A \rangle = \int A(q)P(q) dq. \quad (7)$$

This expression, however, includes the important quantum effects, and the probability density is represented by

$$P(q) = (1/Z)(\mu/2\pi\beta)^{1/2} \exp[-\beta V_L(q)], \quad (8)$$

where the local effective potential $V_L(q)$ is defined by

$$\begin{aligned} \exp[-\beta V_L(q)] &= \int dq' \exp[-V_e(q+q')][2\pi\alpha(q+q')]^{-1/2} \\ &\times \exp[-q^2/2\alpha(q+q')]. \end{aligned} \quad (9)$$

Now we have used the relations

$$V_e(q) \equiv w(q) + (1/\beta) \ln[\sinh f(q)/f(q)], \quad (10)$$

$$f(q) = \beta\omega(q)/2,$$

$$\alpha(q) = [\coth f(q) - 1/f(q)]/[2\mu\omega(q)]. \quad (11)$$

The local effective potential $V_L(q)$ is reduced to the bare potential $V(q)$ in the high-temperature limit. In the EXAFS analyses the operator A should be $\exp(2ik\Delta_\alpha)$, and in the XPD analyses it should be $\exp[2ik\Delta_\alpha(1 - \cos\theta_\alpha)]$ within the plane-wave approximation, where \mathbf{k} is the wavevector of an ejected photoelectron, $k = |\mathbf{k}|$, and Δ_α is the projected relative displacement (Beni & Platzman, 1976) which is simply given by $\Delta q = q - q_0$ (q_0 is the equilibrium interatomic distance) in one-dimensional cases (Tranquada & Ingalls, 1983). θ_α is the scattering angle of the photoelectron by a surrounding atom α . Thus, what we should calculate to study EXAFS thermal factors is the thermal average including the quantum fluctuation given by use of the probability density $P(q)$ defined by (8),

$$\begin{aligned}
g(k) &= \langle \exp(2ikq) \rangle \\
&= \int_{-\infty}^{\infty} \exp(2ikq) P(q) dq = |g(k)| \exp[i\varphi(k)]. \quad (12)
\end{aligned}$$

The XPD thermal factor depends on the scattering angle θ in addition to k ,

$$\begin{aligned}
g(k, \theta) &= \langle \exp[ikq(1 - \cos \theta)] \rangle \\
&= \int_{-\infty}^{\infty} \exp[ikq(1 - \cos \theta)] P(q) dq \\
&= |g(k, \theta)| \exp[i\varphi(k, \theta)], \quad (13)
\end{aligned}$$

in the plane-wave approximation. This factor does not show the thermal damping in the forward direction. If we go beyond the plane-wave thermal approximation, the thermal damping can be expected even in the forward direction (Yanagawa & Fujikawa, 1996*b*; Fujikawa *et al.*, 1998). We now shifted the origin for the potential V to be $q_0 = 0$. This expression clearly shows that the widely used classical real-space representation is reproduced with some modification including the quantum fluctuation effects: the original interatomic potential V should be replaced by the local effective potential $V_L(q)$ which is temperature dependent and tends to $V(q)$ at high temperature from a physical consideration.

When all of the integrals in the cumulants and also the cumulant expansion converge, the thermal damping function $g(k)$ can be written

$$\begin{aligned}
g(k) &= \exp[-2k^2 \langle q^2 \rangle_c + \frac{2}{3} k^4 \langle q^4 \rangle_c - \dots] \\
&\quad \times \exp[i(k \langle q \rangle_c - \frac{4}{3} k^3 \langle q^3 \rangle_c + \dots)]. \quad (14)
\end{aligned}$$

The n th-order moments can be evaluated by

$$\langle q^n \rangle = \int_{-\infty}^{\infty} q^n P(q) dq, \quad (15)$$

and those cumulants are calculated from the lower-order moments,

$$\langle q \rangle_c = \langle q \rangle,$$

$$\langle q^2 \rangle_c = \langle q^2 \rangle - \langle q \rangle^2,$$

$$\langle q^3 \rangle_c = \langle q^3 \rangle - 3\langle q^2 \rangle \langle q \rangle + 2\langle q \rangle^3,$$

$$\langle q^4 \rangle_c = \langle q^4 \rangle - 4\langle q^3 \rangle \langle q \rangle - 3\langle q^2 \rangle^2 + 12\langle q^2 \rangle \langle q \rangle^2 - 6\langle q \rangle^4. \quad (16)$$

In comparison with the results for the symmetric potentials (Fujikawa *et al.*, 1997), the odd orders of the cumulant expansion can contribute to the phase of the thermal damping factor. This expansion is useless for the Morse potential in the high-temperature region because each of the cumulant $\langle q^n \rangle_c$ diverges for this potential, whereas each

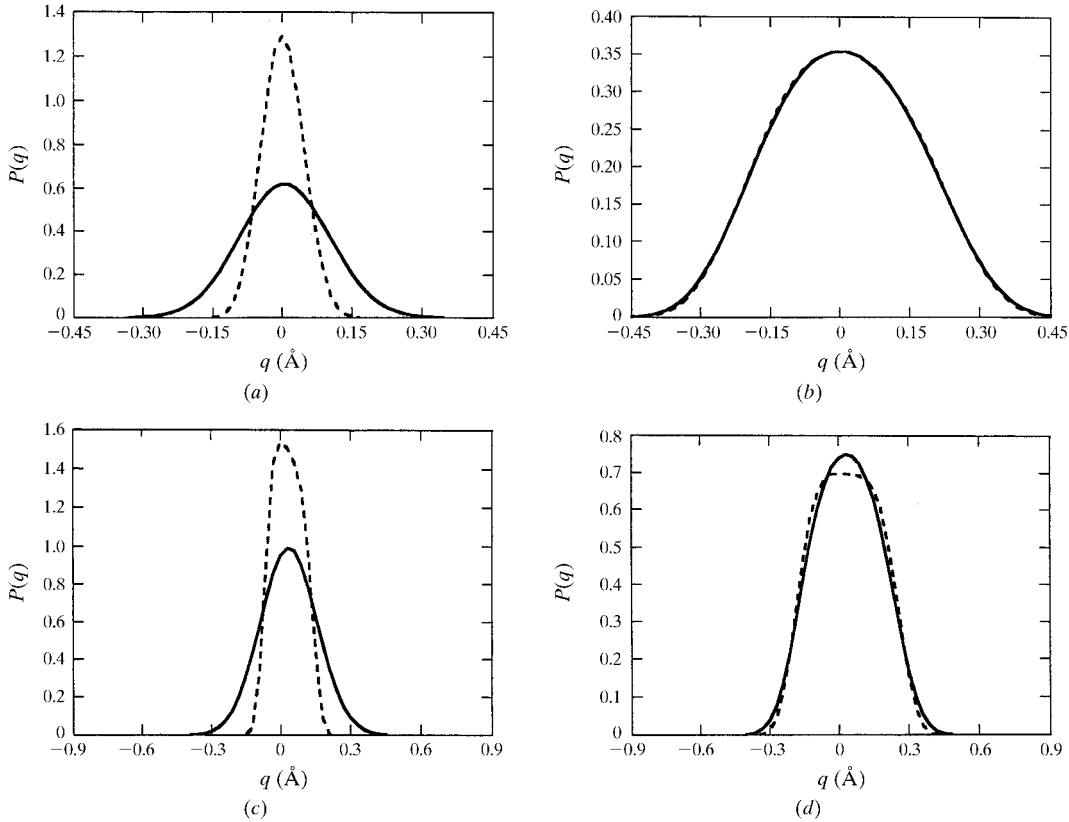


Figure 1

(a) The quantum [solid line, given by equation (8)] and the classical (dashed line) probability density function for the weak anharmonic potential ($a = 0.05$, $b = 0.1$) at $T = 0.1$. (b) The same graph as (a) except for $T = 2.0$. (c) The same graph except for the strong anharmonic potential ($a = 2.5$, $b = 5.0$) at $T = 0.1$. (d) The same graph as (c) except for $T = 2.0$.

cumulant converges for the present anharmonic cubic and quartic potential.

The anharmonic cubic and quartic potential can be represented as

$$V(q) = (\mu\omega_0^2/2)q^2 - \mu a q^3 + \mu b q^4, \quad (17)$$

where μ is the reduced mass, and a and b are parameters which describe the anharmonicity; hereafter we use $a = 0.05$ and $b = 0.1$ for weak anharmonicity and $a = 2.5$ and $b = 5.0$ for strong anharmonicity. In the practical systems it has been reported that $a = 0.32$ and $b = 0.17$ for liquid Pb (Stern *et al.*, 1991), $a = 0.76$ and $b = 0.42$ for Kr crystal (Yokoyama *et al.*, 1997) and $a = 0.714$ and $b = 0.43$ for the Br₂ molecule (Yokoyama, 1998). For the present cubic and quartic potential, $\omega(q)$ and $w(q)$ are given by

$$\omega^2(q) = \omega_0^2 + 12b\alpha(q) - 6aq + 12bq^2, \quad (18)$$

$$w(q) = (\mu\omega_0^2/2)q^2 + \mu b(q^4 - 3\alpha^2) - \mu a q^3. \quad (19)$$

In the numerical calculation, $\mu = \omega_0 = 1$ for simplicity. We consider the two different temperature regions: reduced temperature $T = 0.1$ for low temperature and $T = 2.0$ for high temperature ($T = 1.0$ corresponds to the Einstein temperature). $T = 2.0$ ($T = 0.1$) corresponds to 132 K

(6.6 K) for the Pb–Pb atomic pair (Stern *et al.*, 1991) and $T = 2.0$ ($T = 0.1$) corresponds to 1046 K (52.3 K) for Cu–O (Crozier *et al.*, 1987).

3. Results for EXAFS thermal factors

Figs. 1(a) and 1(b) compare the probability density of the self-consistent result, equation (8), with that of the classical approximation for the weak anharmonic system ($a = 0.05$, $b = 0.1$) at low and high temperature. At low temperature ($T = 0.1$), shown in Fig. 1(a), the probability density from the self-consistent calculation represents the broad peak, whereas that from the classical approximation is given by the narrow peak. This phenomena indicates that the tunnelling effect for the potential well is prominent at low temperature in the self-consistent calculation. In the case of the Morse potential (Miyanaga & Fujikawa, 1998) the peak observed in the self-consistent calculation shifts to larger distance, which arises from the quantum tunnelling effect with a finite potential well. In the case of a cubic and quartic potential, the potential well is infinite and the prominent peak shift cannot be observed. At high temperature ($T = 2.0$), shown in Fig. 1(b), the classical

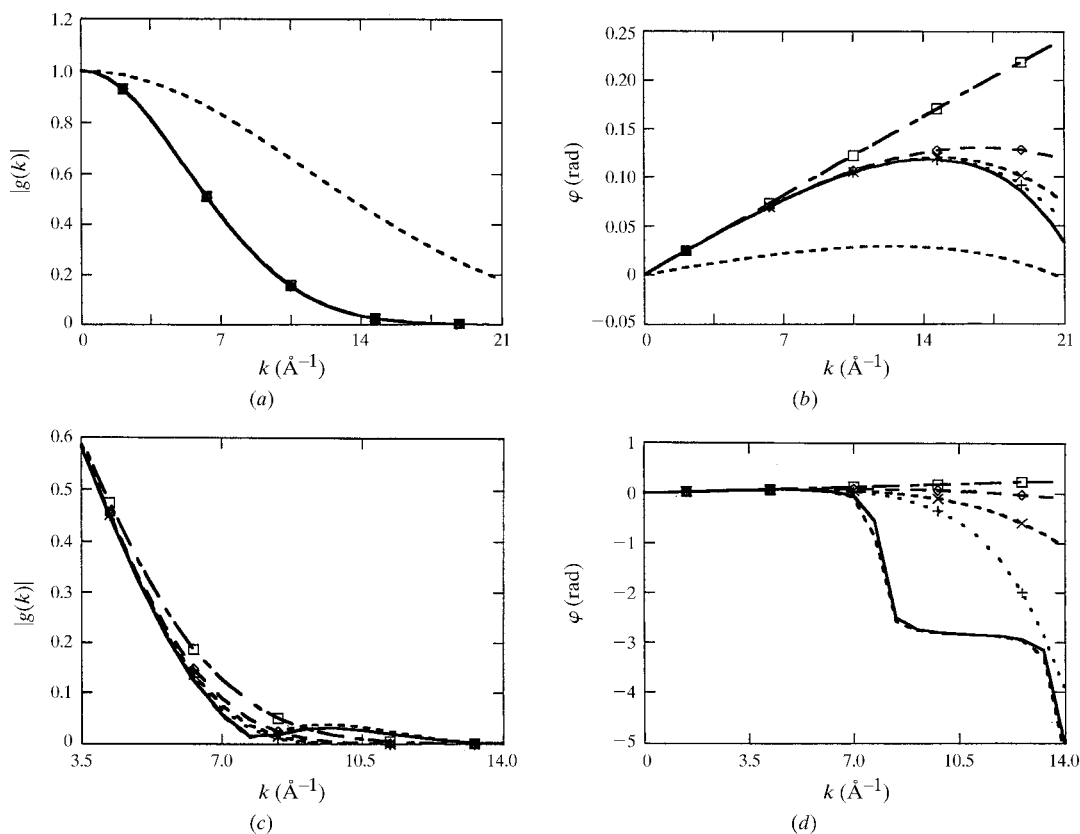


Figure 2

(a) The EXAFS thermal damping function obtained from equation (12) for weak anharmonicity ($a = 0.05$, $b = 0.1$) as a function of k at $T = 0.1$. The solid line shows the quantum calculation and the dashed line shows the classical approximation. The cumulant up to the second-order (squares), fourth-order (diamonds), sixth-order (crosses) and eighth-order (pluses) terms. (b) The EXAFS phase function obtained from equation (12) for weak anharmonicity ($a = 0.05$, $b = 0.1$) as a function of k at $T = 0.1$. The solid line shows the quantum calculation and the dashed line shows the classical approximation. The cumulant up to the first-order (squares), third-order (diamonds), fifth-order (crosses) and seventh-order (pluses) terms. (c) The same graph as (a) except for $T = 2.0$. (d) The same graph as (b) except for $T = 2.0$.

result is quite close to the self-consistent result, and we can expect that the classical approximation works well. A similar result was obtained for the Morse potential (Miyanaga & Fujikawa, 1998).

Figs. 1(c) and 1(d) compare the probability density of the self-consistent result, equation (8), with that of the classical approximation for the strongly anharmonic system ($a = 2.5$, $b = 5.0$) at low ($T = 0.1$) and high ($T = 2.0$) temperature. The peak width of the probability density is narrower than that for weak anharmonicity. At low temperature ($T = 0.1$), shown in Fig. 1(c), the probability density from the self-consistent calculation is broad and shifts to larger distance in comparison with the classical approximation. This result is qualitatively similar to the result observed at high temperature. However, even at high temperature for the strongly anharmonic system the probability density obtained by use of the self-consistent calculation shows the prominent differences from that of the classical approximation, whereas no clear difference has been observed for weak anharmonicity. This interesting result suggests that the quantum effect is prominent for the strongly anharmonic system.

We consider the important parameter g to describe how large the quantum effect is. In the case of the Morse potential,

$$V(q) = D[\exp(-2\Gamma q) - 2\exp(-\Gamma q)], \quad (20)$$

with

$$g = (2\Gamma^2/\mu D)^{1/2}. \quad (21)$$

Small (large) g value gives rise to a weak (strong) quantum effect.

Comparing the third- and fourth-order terms of the power series expansion of the Morse potential,

$$V(q) = -D + D\Gamma^2 q^2 - D\Gamma^3 q^3 + \frac{7}{12}D\Gamma^4 q^4 - \dots, \quad (22)$$

with the present anharmonic potential (17), we obtain D and Γ in terms of $\mu^3\omega_0^6/8a^2$ and $2a/\mu\omega_0^2$. We thus approximately estimate the parameter g by use of (21); $g = 0.71$ for the weakly anharmonic potential and $g = 33.8$ for the strongly anharmonic one. This means that the quantum effect is large for the strongly anharmonic potential. As shown in Figs. 1(b) and 1(d), the classical approximation is poor even at high temperature for the strongly anharmonic

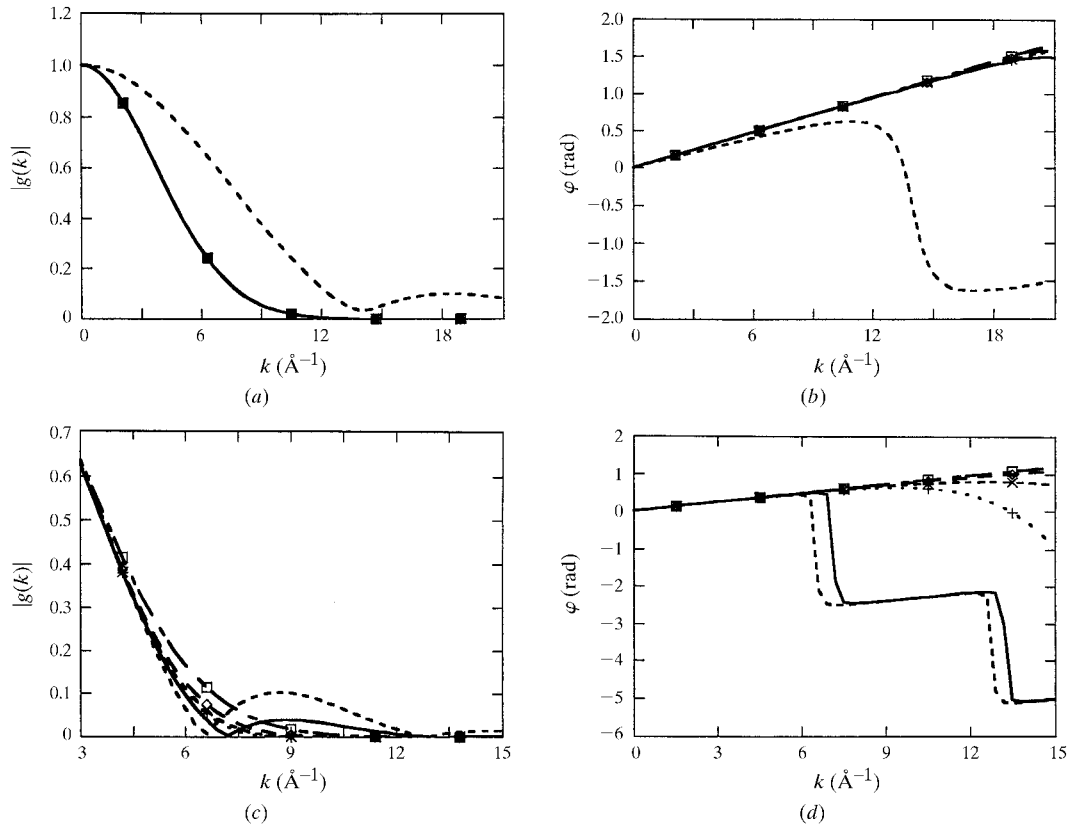


Figure 3

(a) The EXAFS thermal damping function obtained from equation (12) for strong anharmonicity ($a = 2.5$, $b = 5.0$) as a function of k at $T = 0.1$. The solid line shows the quantum calculation and the dashed line shows the classical approximation. The cumulant up to the second-order (squares), fourth-order (diamonds), sixth-order (crosses) and eighth-order (pluses) terms. (b) The EXAFS phase function obtained from equation (12) for strong anharmonicity ($a = 2.5$, $b = 5.0$) as a function of k at $T = 0.1$. The solid line shows the quantum calculation and the dashed line shows the classical approximation. The cumulant up to the first-order (squares), third-order (diamonds), fifth-order (crosses) and seventh-order (pluses) terms. (c) The same graph as (a) except for $T = 2.0$. (d) The same graph as (b) except for $T = 2.0$.

potential, which is quite in contrast to the weakly anharmonic potential.

Figs. 2(a) and 2(b) show the amplitude $|g(k)|$ and the phase $\varphi(k)$ of the EXAFS thermal factor, respectively, defined by (12) at low temperature ($T = 0.1$) for the weakly anharmonic system ($a = 0.05$, $b = 0.1$). This figure shows the results from the self-consistent calculation compared with the classical approximation and the cumulant approximation defined by (14)–(16) [up to the second-, fourth-, sixth- and eighth-order terms for the amplitude (a) and up to the first, third, fifth and seventh terms for the phase (b)]. In Fig. 2(a) the cumulant expansion up to the second-order term gives quite a satisfactory result for the amplitude, *i.e.* it shows a good agreement with the self-consistent calculation, whereas the classical approximation gives a poor result. In Fig. 2(b) for the phase, the first-order cumulant gives a linear function of k , which is a poor approximation, whereas the cumulant expansion up to the seventh-order term gives quite a satisfactory agreement. We also observed the slow convergence for the phase factor in the cumulant expansion in the study of the thermal damping factor for the Morse potential (Miyanaga & Fujikawa, 1998).

Figs. 2(c) and 2(d) show the amplitude and phase, respectively, of the EXAFS thermal factor at high

temperature ($T = 2.0$) for the weakly anharmonic system ($a = 0.05$, $b = 0.1$). The amplitude is negative at $8 < k < 13 \text{ \AA}^{-1}$, so that the phase of $g(k)$ changes about π discontinuously at $k = 8 \text{ \AA}^{-1}$. At such a high temperature the classical approximation works well; however, the cumulant approximation is poor even for weakly anharmonic systems because it cannot predict rapid change of $|g(k)|$ and $\varphi(k)$ near $k = 8 \text{ \AA}^{-1}$. The convergence is very slow for the cumulant expansion at $10 < k < 14 \text{ \AA}^{-1}$ (this is significant in the practical EXAFS analyses). This singular behaviour is in contrast to the smooth change of $|g(k)|$ and $\varphi(k)$ observed at low temperature in Figs. 2(a) and 2(b).

Figs. 3(a) and 3(b) show the amplitude and phase of the EXAFS thermal factor, respectively, at low temperature ($T = 0.1$) for the strongly anharmonic system ($a = 2.5$, $b = 5.0$). The thermal reduction (attenuation) of the amplitude for the strongly anharmonic system is smaller than that for the weakly anharmonic system. The cumulant expansion shows good convergence for the strong anharmonicity; this observation is quite similar to the weakly anharmonic systems in Figs. 2(a) and 2(b). The phase $\varphi(k)$ for the strongly anharmonic system shows a monotonic increase up to about $k = 20 \text{ \AA}^{-1}$, whereas that for the weakly anharmonic system decreases in the region $k > 14 \text{ \AA}^{-1}$, shown in

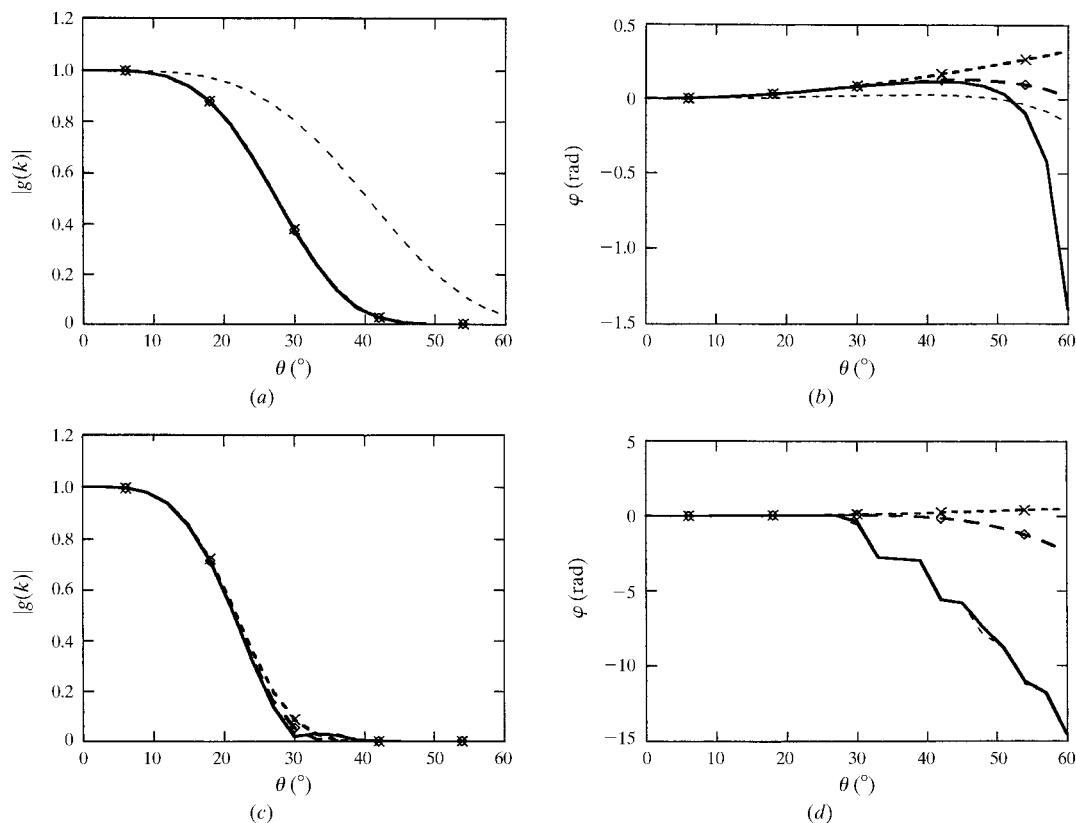


Figure 4

(a) The XPD thermal damping function obtained from equation (13) for weak anharmonicity ($a = 0.05$, $b = 0.1$) as a function of θ at $T = 0.1$. The energy of the photoelectron is 1000 eV. The solid line shows the quantum calculation and the dashed line shows the classical approximation. The cumulant up to the second-order (crosses) and fourth-order (diamonds) terms. (b) The XPD phase function obtained from equation (13) for weak anharmonicity ($a = 0.05$, $b = 0.1$) as a function of θ at $T = 0.1$. The solid line shows the quantum calculation and the dashed line shows the classical approximation. The cumulant up to the first-order (crosses) and third-order (diamonds) terms. (c) The same graph as (a) except for $T = 2.0$. (d) The same graph as (b) except for $T = 2.0$.

Fig. 2(b). The cumulant expansion shows rapid convergence in comparison with that for the weakly anharmonic system shown in Figs. 2(a) and 2(b). This behaviour is related to g ; for large g (strong quantum effect) the convergence of the cumulant expansion is generally rapid. The classical approximation is poor as expected for the low-temperature region.

Figs. 3(c) and 3(d) show the amplitude and phase, respectively, of the EXAFS thermal factor at high temperature ($T = 2.0$) for the strongly anharmonic system ($a = 2.5$, $b = 5.0$). The amplitude $|g(k)|$ shows the negative value at $7.5 < k < 12 \text{ \AA}^{-1}$ and phase shifts about π as shown in Figs. 2(c) and 2(d). The amplitude $|g(k)|$ and the phase $\varphi(k)$ show a rapid change in the region $k = 6\text{--}7.5 \text{ \AA}^{-1}$ for the self-consistent and the classical approaches, whereas the cumulant expansion gives a smooth change as expected. The classical result is similar to that of the self-consistent calculation; however, the agreement with the self-consistent calculation is worse than that for the weakly anharmonic system shown in Figs. 2(c) and 2(d). This behaviour is explained by the strong anharmonicity which is expected to show the strong quantum effect as discussed before; even at high temperature the quantum effects play some important roles.

4. Results for XPD thermal factors

In this section we discuss the XPD thermal factors with cubic and quartic anharmonicity. In the analyses of XPD spectra, small-angle scattering plays an important role and so we calculate the thermal factor up to $\theta = 60^\circ$. The kinetic energy of the photoelectron is assumed to be 1000 eV; our attention will be focused on the angular distribution of XPD intensity at high energy.

Figs. 4(a) and 4(b) show the amplitude $|g(\theta)|$ and phase $\varphi(\theta)$, respectively, of the XPD thermal factor defined by (13) as a function of the scattering angle θ at low temperature ($T = 0.1$) for the weakly anharmonic system ($a = 0.05$, $b = 0.1$). The self-consistent calculation is compared with the classical approximation and the cumulant approximation defined by (14)–(16) [up to the second- and fourth-order terms for amplitude (a) and up to the first and third terms for phase (b)]. In Fig. 4(a) the cumulant expansion up to the second order gives quite a good result for the amplitude as observed in the case of the Morse potential (Miyanaga & Fujikawa, 1998), whereas in Fig. 4(b) the cumulant expansion shows rather slow convergence. The classical approximation is very poor for the amplitude and the phase as shown in the EXAFS thermal factor.

Figs. 4(c) and 4(d) show the amplitude and phase, respectively, of the XPD thermal factor at high temperature ($T = 2.0$) for the weakly anharmonic system ($a = 0.05$, $b = 0.1$). In Fig. 4(c) both the cumulant and the classical approximations give rather good results in the small-angle region $\theta < 30^\circ$. In the large-angle region, $\theta > 30^\circ$, the disagreement between the self-consistent calculation and

the cumulant expansion is prominent, particularly for the phase. The classical approximation shows good results even for the large-angle scattering. These results can be compared with those shown in Figs. 2(c) and 2(d), where we have found quite similar results. Under other conditions discussed for the EXAFS thermal factors we obtain very similar results to those obtained for the EXAFS thermal factors. We will not repeat the similar discussion.

5. Conclusions

We have studied the thermal effects in EXAFS and X-ray photoelectron diffraction spectra due to atomic vibration with cubic and quartic anharmonicity by use of Feynman's path-integral approach. This approach can be applied to strongly anharmonic systems where the cumulant analyses break down, and it is closely related to the well known classical approach which is only valid at high temperature.

Some pronounced different features are observed for this asymmetric potential in comparison with the results for the symmetric potentials where only thermal damping is expected. The phase of the thermal factor plays an important role both in EXAFS and XPD analyses. At low temperature the cumulant expansion up to the second order agrees well with the self-consistent result for $|g(k)|$, but up to the fifth- or seventh-order cumulant should be taken into account for the phase function $\varphi(k)$ for EXAFS analyses. At high temperature the result from self-consistent calculations shows the characteristic behaviour; the rapid change of the phase cannot be explained by the low-order cumulant expansion.

We compared the two different cases: the strong and the weak quantum effects. For weak anharmonicity the classical approximation is good over a wide temperature region; however, for strong anharmonicity it is poor because of strong quantum effects. The parameter g is important for such a qualitative discussion.

References

- Arvanitis, D., Lederer, T., Comelli, G., Tischer, M., Yokoyama, T., Troger, L. & Baberschke, K. (1993). *Jpn. J. Appl. Phys.* **S32**(2), 337–339.
- Beni, G. & Platzman, P. M. (1976). *Phys. Rev. B*, **14**, 1514–1518.
- Brouder, C. (1988). *J. Phys. C*, **21**, 5075–5086.
- Brouder, C. & Goulon, J. (1989). *Physica B*, **158**, 351–354.
- Crozier, E. D., Alberding, N., Bauchspiess, K. R., Seary, A. J. & Gygax, S. (1987). *Phys. Rev. B*, **36**, 8288–8293.
- Cucoli, A., Giachetti, R., Tognetti, V., Vaia, R. & Verrucchi, P. (1995). *J. Phys. Condens. Matter*, **7**, 7891–7938.
- Dalba, G., Fornasini, P., Grazioli, M., Gotter, R. & Rocca, F. (1995). *Physica B*, **208/209**, 135–136.
- Dalba, G., Fornasini, P., Grazioli, M., Pasqualini, D., Diop, D. & Monti, F. (1998). *Phys. Rev. B*, **58**, 4793–4802.
- Feynman, R. P. (1972). *Statistical Mechanics*. Reading, MA: Benjamin.
- Feynman, R. P. & Kleinert, H. (1986). *Phys. Rev. A*, **34**, 5080–5084.
- Frenkel, A. I. & Rehr, J. J. (1993). *Phys. Rev. B*, **48**, 585–588.

- Fujikawa, T. & Miyanaga, T. (1993). *J. Phys. Soc. Jpn*, **62**, 4108–4122.
- Fujikawa, T., Miyanaga, T. & Suzuki, T. (1997). *J. Phys. Soc. Jpn*, **66**, 2897–2906.
- Fujikawa, T., Nakayama, K. & Yanagawa, T. (1998). *J. Electron Spectrosc. Relat. Phenom.* **88/91**, 527–531.
- Fujikawa, T., Yimaga, M. & Miyanaga, T. (1995). *J. Phys. Soc. Jpn*, **64**, 2047–2068.
- Ishii, T. (1992). *J. Phys. Condens. Matters*, **4**, 8029–8034.
- Miyanaga, T. & Fujikawa, T. (1994a). *J. Phys. Soc. Jpn*, **63**, 1036–1052.
- Miyanaga, T. & Fujikawa, T. (1994b). *J. Phys. Soc. Jpn*, **63**, 3683–3690.
- Miyanaga, T. & Fujikawa, T. (1998). *J. Phys. Soc. Jpn*, **67**, 2930–2937.
- Mustre de Leon, J., Conradson, S. D., Batistic, I., Bishop, A. R., Raistrick, I. D., Aronson, M. C. & Garzon, F. H. (1992). *Phys. Rev. B*, **45**, 2447–2457.
- Rabus, H., Arvanitis, D., Lederer, T. & Baberschke, K. (1991). *X-ray Absorption Fine Structure*, edited by S. S. Hasnain, pp. 193–199. New York: Ellis Horwood.
- Rennert, P. (1992). *J. Phys. Condens. Matter*, **4**, 4315–4322.
- Rennert, P. (1993). *Jpn. J. Appl. Phys.* **S32(2)**, 19–21.
- Stern, E. A., Livins, P. & Zhang, Z. (1991). *Phys. Rev. B*, **43**, 8850–8860.
- Tranquada, J. M. & Ingalls, R. (1983). *Phys. Rev. B*, **28**, 3520–3528.
- Yanagawa, T. & Fujikawa, T. (1996a). *J. Phys. Soc. Jpn*, **65**, 1832–1843.
- Yanagawa, T. & Fujikawa, T. (1996b). *Surf. Sci.* **357/358**, 125–130.
- Yimaga, M. & Fujikawa, T. (1996). *J. Electron Spectrosc.* **79**, 29–32.
- Yokoyama, T. (1998). *Phys. Rev. B*, **57**, 3423–2432.
- Yokoyama, T., Kobayashi, K., Ohta, T. & Ugawa, A. (1996a). *Phys. Rev. B*, **53**, 6111–6122.
- Yokoyama, T., Kobayashi, K., Ohta, T. & Ugawa, A. (1996b). *Phys. Rev. B*, **54**, 6921–6928.
- Yokoyama, T., Ohta, T. & Sato, H. (1997). *Phys. Rev. B*, **55**, 11320–11329.
- Yokoyama, T., Satsukawa, T. & Ohta, T. (1989). *Jpn. J. Appl. Phys.* **28**, 1905–1908.